Appl Phys A (2011) 104:129–133
DOI 10.1007/s00339-010-6080-7

Applied Physics A
Materials Science & Processing

Dielectric and polar order behaviors of $BaTiO_3$-$Bi(Mg_{1/2}Ti_{1/2})O_3$ ceramics

Ruiting Sun · Xiaoli Wang · Jing Shi · Le Wang

Received: 10 May 2010 / Accepted: 6 October 2010 / Published online: 21 October 2010

Abstract New perovskite solid solution ceramics of $(1-x)BaTiO_3$-$xBi(Mg_{1/2}Ti_{1/2})O_3$ ($(1-x)$BT-xBMT, $x \leq 0.09$) were synthesized by the solid-state reaction technique. X-ray diffraction studies have revealed a stable single perovskite structure for all samples. Dielectric measurements were carried out at different frequencies and temperatures. The polarization evolutions with temperatures were measured to investigate the ferroelectric properties. All the compositions show features of ferroelectrics with diffuse phase transition, though the temperature T_m of their dielectric constant maximum ε_m is frequency dependent. The dielectric constant peak $\varepsilon(T)$ of $(1-x)$BT-xBMT ceramics become broad with increasing BMT content. During the temperature range of $\varepsilon(T)$ peak summit, $(1-x)$BT-xBMT ceramics present quasi-linear dielectric phenomenon under high electric field with very high dielectric constant.

1 Introduction

$BaTiO_3$-based ceramics have been widely used in electronic industry, ranging from high-permittivity capacitors to microwave tunable devices, positive temperature coefficient resistors, and piezoelectric transducers. The $BaTiO_3$-based dielectrics usually display a remarkable dielectric nonlinearity, that is, the dielectric constant is a function of external electric field [1–6]. This behavior limits the application area. For instance, these dielectrics are not suitable in the occasions under high electric field or field intensity variation. For most ferroelectrics, high dielectric constant and dielectric linearity are contradictory.

In order to explore new ferroelectric materials, many Bi-based complex perovskites have been investigated, such as $(Bi_{1/2}Na_{1/2})TiO_3$ [7, 8], $(Bi_{1/2}K_{1/2})TiO_3$ [9], $Bi(Zn_{1/2}Ti_{1/2})O_3$ [10], $Bi(Mg_{1/2}Ti_{1/2})O_3$ [11], $(Bi_{3/4}Na_{1/4})(Mg_{1/4}Ti_{3/4})O_3$, and $(Bi_{3/4}K_{1/4})(Mg_{1/4}Ti_{3/4})O_3$ [12] etc. The solid solutions of $BaTiO_3$ or $PbTiO_3$ with some Bi-based perovskites are also reported [13–18]. A special phenomenon of dielectric quasi-linearity under high electric field was observed in two solid solution system ceramics of $BaTiO_3$-$(Bi_{3/4}Na_{1/4})(Mg_{1/4}Ti_{3/4})O_3$ and $BaTiO_3$-$Bi(Zn_{1/2}Ti_{1/2})O_3$ [17, 18]. In this article, we synthesized $BaTiO_3Bi(Mg_{1/2}Ti_{1/2})O_3$ perovskite solid solutions with $Bi(Mg_{1/2}Ti_{1/2})O_3$ content less than 10 mol%, and investigated their dielectric and ferroelectric properties.

2 Experimental

Ceramics of $(1-x)BaTiO_3$-$xBi(Mg_{1/2}Ti_{1/2})O_3$[$(1-x)$BT-xBMT] with $x = 0.05$, 0.07, and 0.09 were synthesized by solid-state reaction technique. Stoichiometric amounts of reagent grade oxide powders of Bi_2O_3, MgO, TiO_2, and $BaCO_3$ were wet mixed by ball milling. The dried powders were pre-sintered in covered crucibles at 900°C for 2 h. Then the pre-sintered powders were wet ball milled. The dried powders were mixed with a 5% PVA binder and were pressed into 12.7 mm diameter and ∼1 mm thick pellets under a pressure of 2 MPa. Following binder burned out at 500°C for 5 h, the pellets were sintered in a sealed crucible at temperatures ranging between 1300 and 1350°C for 3 h.

Crystal structures of the ceramic samples were detected using a Rigaku D/max 2400 X-ray diffractometer (XRD) with CuK_α radiation. For dielectric measurements, ceramic

R. Sun · X. Wang (✉) · J. Shi · L. Wang
MOE Key Laboratory for Nonequilibrium Synthesis and Modulation of Condensed Matter, School of Science, Xi'an Jiaotong University, Xi'an 710049, China
e-mail: xlwang1@mail.xjtu.edu.cn

samples were polished to obtain smooth and parallel surfaces, and then painted with silver paste as electrodes after being fired at 810°C for 10 min. The dielectric constant ε and dielectric loss tanδ were measured on an automated system, within a temperature control sample chamber and an Agilent 4284A inductance-capacitance-resistance (LCR) meter controlled by a personal computer. The heating rate was 2°C/min. For ferroelectric hysteresis loop measurements, a sinusoidal signal of 1 Hz, generated by a personal computer with a PCI6221 Data Acquisition (DAQ) card, was applied to the sample after it was amplified through a Trek 610E high-voltage supply/amplifier/controller. The current through the sample was collected by the DAQ card, and converted to digital signal wherein. The hysteresis loop was obtained through polarization current integration with time.

3 Results and discussion

Figure 1 shows the XRD patterns for $(1-x)$BT-xBMT ceramics at room temperature. All the reflection peaks could be indexed based on perovskite structure and no second phase is observed within the detection limit of XRD. The full width at half maximum of the reflection peaks (200) of the solid solutions is as wide as that of the reflection peaks (002) and (200) of parent $BaTiO_3$ ceramic. The difference is that the peak splitting between the reflection planes (200) and (002) of tetragonal symmetry becomes more and more feint with increasing BMT content. Combining their dielectric properties represented later, the three solid solution ceramics are mixture of tetragonal (T) and cubic (C) perovskite phases at room temperature. The ratio of T/C declines with increasing x.

Figure 2 shows the temperature dependence of dielectric constant ε and dielectric loss tanδ of $(1-x)$BT-xBMT ceramics measured at different frequencies. The temperature T_m of the maximum dielectric constant ε_m decreases and becomes more frequency dependent with increasing BMT content. The values of ΔT_m $(=T_{m,100\text{ kHz}} - T_{m,0.1\text{ kHz}})$ for the compositions with $x = 0.05$, 0.07 and 0.09 are 1, 11 and 35°C, respectively. Composition 0.91BT-0.09BMT shows a rather broad $\varepsilon(T)$ peak in contrast with the other two ceramics. The broad dielectric peak of 0.91BT-0.09BMT is in the vicinity of room temperatures and highly frequency dependent. When temperature reaches 120°C, it turns frequency-independent. The ε obeys the Curie-Weiss law at above 120°C,

$$\varepsilon = C/(T - T_{CW}), \tag{1}$$

where C is the Curie constant, and T_{CW} is the Curie–Weiss temperature. The Curie–Weiss law accounted for the phonon

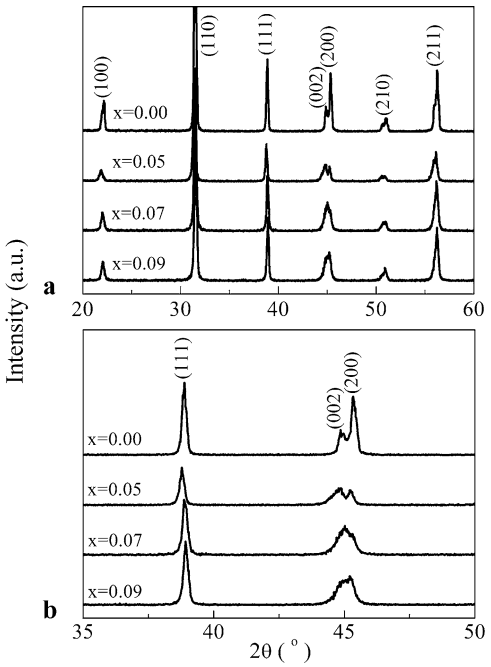

Fig. 1 X-ray diffraction patterns (**a**) and the {200} peak splittings (**b**) for $(1-x)$BT-xBMT ceramics with $x = 0$, 0.05, 0.07 and 0.09 at room temperature

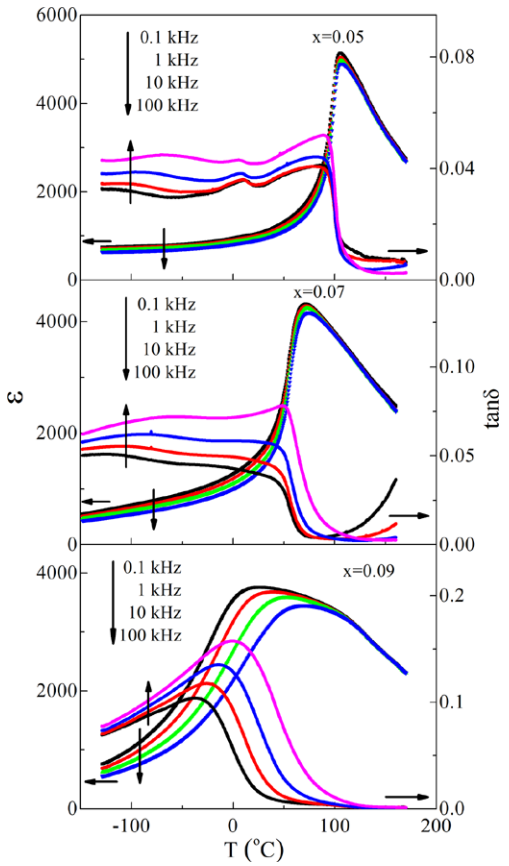

Fig. 2 Temperature dependence of dielectric constant ε and dielectric loss tanδ at different frequencies for $(1-x)$BT-xBMT with $x = 0.05$, 0.07, and 0.09

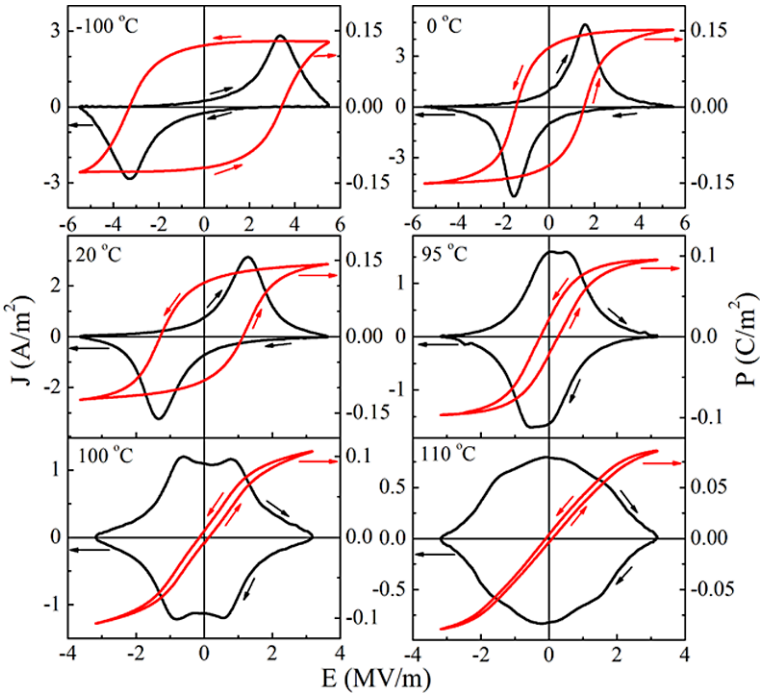

Fig. 3 Electric field dependence of the polarization current density J and polarization P at different temperatures for the 0.95BT-0.05BMT sample

polarization, which fits only for the high temperature slope of $\varepsilon(T)$. It is reasonable to believe that 120°C is the Burns temperature T_B for 0.91BT-0.09BMT [19, 20]. Accordingly, there might be $BaTiO_3$ or rich-$BaTiO_3$ polar nanoregions in the grains of 0.91BT-0.09BMT ceramics.

The electric field E dependence of polarization current density J and polarization P at different temperatures for 0.95BT-0.05BMT ceramic is plotted in Fig. 3. There is an electric current peak with increasing external voltage in a normal ferroelectric, which indicates the reverse of domains. In the BT-BMT ceramics, the evolution of $J(E)$ loops with temperatures is complex. Besides a J peak with increasing E, there is a J peak with decreasing E in some range of the temperature. In order to describe this clearly, based on the normal physical concepts of charge and discharge current density, we use "charge current density" to indicate the current density with increasing field, and "discharge current density" the current density with decreasing field for sinusoidal signal. The composition of 0.95BT-0.05BMT presents a normal ferroelectric hysteresis loop around and below room temperatures. The coercive field E_c rises observably upon cooling, from 1.28 MV/m at 20°C to 3.3 MV/m at −100°C. Below 0°C, the remanent polarization P_r stays at 0.12 C/m^2. Above 0°C, P_r decreases from 0.12 to 0.003 C/m^2 at 110°C on heating. At 95°C, the $J(E)$ peak is composed of charge and discharge parts, and the peak top becomes flat. Since the charge part takes the most portion of the peak, the corresponding $P(E)$ curve presents a slim hysteresis loop. With further increasing temperature, the charge and discharge peaks in $J(E)$ loop become more and more clear. It demonstrates that there exist either induced polar order regions or the extension of polar order regions. When the temperature reaches 110°C, the charge and discharge peaks become weaker and move towards opposite sides, meanwhile new broad $J(E)$ peaks around zero external field appear. The corresponding hysteresis loop is close to linearity.

The $J(E)$ and corresponding $P(E)$ loops of 0.93BT-0.07BMT ceramic at different temperatures are represented in Fig. 4. The variation of $J(E)$ loops with temperatures for 0.93BT-0.07BMT is somewhat analogous to that of 0.95BT-0.05BMT. The difference is that the external field of the quasi-linear dielectric response of 0.93BT-0.07BMT becomes higher, and the temperature range where the quasi-linear dielectric behavior takes place under high field becomes wider. Above 90°C, there is no polarization hysteresis behavior, and 0.93BT-0.07BMT presents a paraelectric characteristic. Apparently, the polarization quasi-linear response with external field takes place when there are no domains in the samples, and the polar nanoregions or paraelectric states can be induced into domains under high external field.

Figure 5 represents the $J(E)$ and $P(E)$ loops of 0.91BT-0.09BMT ceramic. Although the composition exhibits a ferroelectric hysteresis loop below −50°C, the $J(E)$ loops at different temperatures tell the variations of polar orders. The shape of the $J(E)$ loop at −110°C is canonical ferroelectric. When temperature increases to −70°C, the $J(E)$ charge peak breaks into two peaks. Meanwhile, the discharge J enlarges, and becomes part of the $J(E)$ peak. It illustrates that the domains could be divided into two sorts

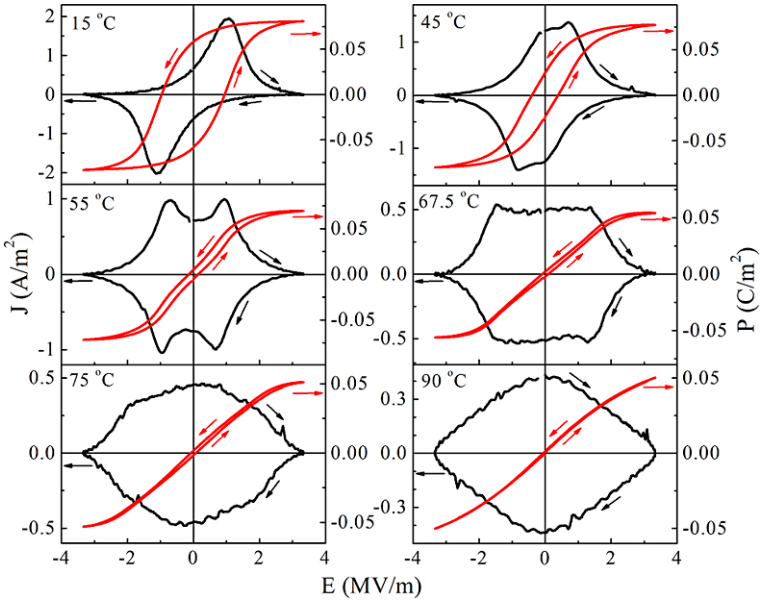

Fig. 4 Electric field dependence of the polarization current density J and polarization P at different temperatures for the 0.93BT-0.07BMT sample

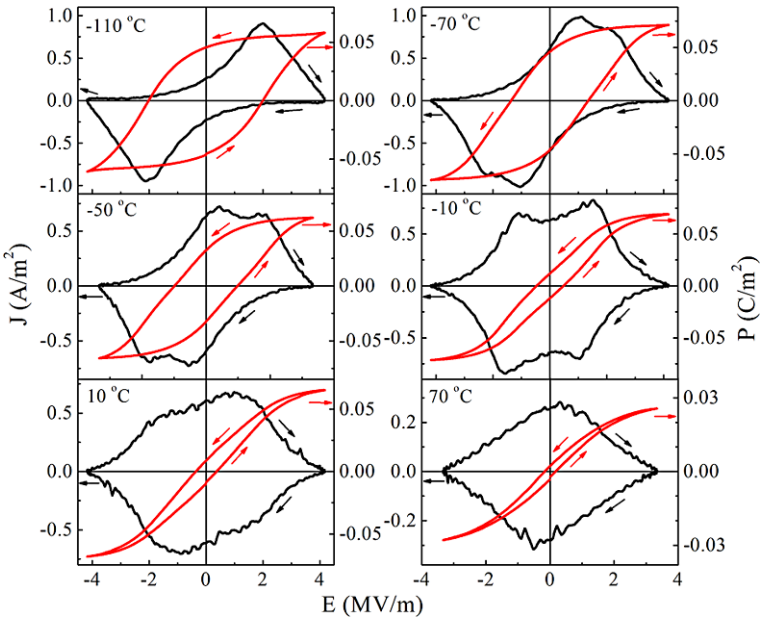

Fig. 5 Electric field dependence of the polarization current density J and polarization P at different temperatures for the 0.91BT-0.09BMT sample

based on their average E_c. The domains with lower E_c break down firstly with heating up. Upon further heating, the $J(E)$ peak changes like the other two compositions as explained above.

The $J(E)$ loops of the three BT-BMT compositions display charge and discharge peaks around their respective $\varepsilon(T)$ peak top area, which indicates a characteristic of field-induced polarization order transition. The charge peak could be caused by the field-induced transition from polar nanoregions or paraelectric states to domains, whereas the discharge peak corresponds to the dissolution of the induced domains. With increasing BMT content, the ferroelectricity of BT-BMT solid solutions weakens, and the $\varepsilon(T)$ peak broadens.

In BT-BMT solid solution ceramics, the Ti^{4+} ions are ferroelectric active, but the Mg^{2+} ions are not. The content ratio of tetragonal phase versus cubic phase at room temperature declines with increasing BMT content. The crystal structural symmetry of the BT matrix in BT-BMT ceramics is not changed by the existence of Mg^{2+} ions with $x \leq 0.07$. The existence of Mg^{2+} ions obviously lowers the transition temperature between ferroelectric and paraelectric phases of BT-BMT ceramics when the content of Mg^{2+} ions $\geq$4.5 mol% ($x \geq 0.09$).

The evolution of the polar order with temperatures for the three ceramics can be estimated according to the relationship of remanent polarization P_r versus temperature depen-

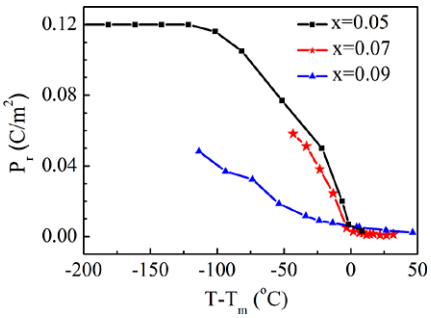

Fig. 6 T–T_m dependence of P_r for $(1-x)$BT-xBMT with $x = 0.05$, 0.07, and 0.09

dence T–$T_{m,0.1\ \mathrm{kHz}}$ is shown in Fig. 6. In temperature range of 50°C above their respective $T_{m,0.1\ \mathrm{kHz}}$, all three compositions keep small P_r between 0.001 and 0.003 C/m^2. In temperature range of 50°C below $T_{m,0.1\ \mathrm{kHz}}$, P_r of 0.95BT-0.05BMT and 0.93BT-0.07BMT ascends quickly in similar rates on cooling, while the increase of P_r for 0.91BT-0.09BMT is relatively much slower.

4 Conclusions

Perovskite ceramics of $(1-x)BaTiO_3$-$xBi(Mg_{1/2}Ti_{1/2})O_3$ ($x \leq 0.09$) were synthesized using oxide mixing process. The $\varepsilon(T)$ peak of the solid solution ceramics becomes broad and T_m decreases with increasing BMT content. All the three compositions are in long ferroelectric polar order in temperatures below the $\varepsilon(T)$ peak area, and the $\varepsilon(T)$ peak might be associated with the transition among macrodomains and polar nanoregions, ferroelectric phase and paraelectric phase. In the temperature range of $\varepsilon(T)$ peak summit, $(1-x)$BT-xBMT ceramics present a quasi-linear dielectric phenomenon under high electric field with very high dielectric constant.

Acknowledgements This work was supported by the Funds of National Natural Science Foundation of China (project no 50772087).

References

1. J. Zhang, J. Zhai, X. Chou, J. Shao, X. Lu, X. Yao, Microwave and infrared dielectric response of tunable $Ba_{1-x}Sr_xTiO_3$ ceramics. Acta Mater. **57**, 4491–4499 (2009)
2. J. Jeon, Effect of $SrTiO_3$ concentration and sintering temperature on microstructure and dielectric constant of $Ba_{1-x}Sr_xTiO_3$. J. Eur. Ceram. Soc. **24**, 1045–1048 (2004)
3. S. Marković, M. Mitrić, N. Cvjetićanin, D. Uskoković, Preparation and properties of $BaTi_{1-x}Sn_xO_3$multilayered ceramics. J. Eur. Ceram. Soc. **27**, 505–509 (2007)
4. L. Wang, X. Wang, Evolution of polar order in $Ba(Ti_{1-x}Sn_x)O_3$ ceramics. Solid State Commun. **149**, 1877–1880 (2009)
5. T. Maiti, R. Guo, A.S. Bhalla, Electric field dependent dielectric properties and high tunability of $BaZr_xTi_{1-x}O_3$ relaxor ferroelectrics. Appl. Phys. Lett. **89**, 122909 (2006)
6. C. Ang, Z. Jing, Z. Yu, Ferroelectric relaxor $Ba(Ti,Ce)O_3$. J. Phys., Condens. Matter **14**, 8901–8912 (2002)
7. J. Suchanicz, J.P. Mercurio, S. Said, B. Garbarz-Glos, Effect of axial pressure on electric properties of Pb-modified $Na_{0.5}Bi_{0.5}TiO_3$ ceramic. Phys. Status Solidi A **193**, 179–186 (2002)
8. P. Setasuwon, N. Vaneesorn, S. Kijamnajsuk, A. Thanaboonsombut, Nanocrystallization of $Bi_{0.5}Na_{0.5}TiO_3$ piezoelectric material. Sci. Technol. Adv. Mater. **6**, 278–281 (2005)
9. Z.F. Li, C.L. Wang, W.L. Zhong, J.C. Li, M.L. Zhao, Dielectric relaxor properties of $K_{0.5}Bi_{0.5}TiO_3$ ferroelectrics prepared by sol–gel method. J. Appl. Phys. **94**, 2548 (2003)
10. M.R. Suchomel, A.M. Fogg, M. Allix, H. Niu, J.B. Claridge, M.J. Rosseinsky, Bi_2ZnTiO_6: a lead-free closed-shell polar perovskite with a calculated ionic polarization of 150 μC cm^{-2}. Chem. Mater. **18**, 4987–4989 (2006)
11. D.D. Khalyavin, A.N. Salak, N.P. Vyshatko, A.B. Lopes, N.M. Olekhnovich, Crystal structure of metastable perovskite $Bi(Mg_{1/2}Ti_{1/2})O_3$: Bi-based structural analogue of antiferroelectric $PbZrO_3$. Chem. Mater. **18**, 5104–5110 (2006)
12. X. Wang, W. Cao, Dielectric properties of new perovskite ceramics $(Na_{1/4}Bi_{3/4})(Mg_{1/4}Ti_{3/4})O_3$ and $(K_{1/4}Bi_{3/4})(Mg_{1/4}Ti_{3/4})O_3$. J. Eur. Ceram. Soc. **27**, 2481–2484 (2007)
13. Y.-M. Chiang, G.W. Farrey, A.N. Soukhojak, Lead-free high-strain single-crystal piezoelectrics in the alkaline–bismuth–titanate perovskite family. Appl. Phys. Lett. **73**, 3683–3685 (1998)
14. J. Shieh, K.C. Wu, C.S. Chen, Switching characteristics of MPB compositions of $(Bi_{0.5}Na_{0.5})TiO_3$–$BaTiO_3$–$(Bi_{0.5}K_{0.5})TiO_3$ lead-free ferroelectric ceramics. Acta Mater. **55**, 3081–3087 (2007)
15. X.D. Zhang, D. Kwon, B.G. Kim, Structural evolution of a high T_c ferroelectric $(x)Bi(Zn_{1/2}Ti_{1/2})O_3$–$(1-x)PbTiO_3$ solid solution. Appl. Phys. Lett. **92**, 082906 (2008)
16. C.A. Randall, R. Eitel, B. Jones, T.R. Shrout, D.I. Woodward, I.M. Reaney, Investigation of a high T_c piezoelectric system: $(1-x)Bi(Mg_{1/2}Ti_{1/2})O_3$–$(x)PbTiO_3$. J. Appl. Phys. **95**, 3633–3639 (2004)
17. X. Wang, W. Cao, Dielectric and ferroelectric properties of $BaTiO_3$–$(Na_{1/4}Bi_{3/4})(Mg_{1/4}Ti_{3/4})O_3$ ceramics. Appl. Phys. Lett. **90**, 042913 (2007)
18. X. Wang, A. Yang, Dielectric and ferroelectric properties of $(Bi_xBa_{1-x})(Zn_{x/2}Ti_{1-x/2})O_3$ ceramics. J. Phys. D, Appl. Phys. **42**, 075419 (2009)
19. A.A. Bokov, Z.-G. Ye, Recent progress in relaxor ferroelectrics with perovskite structure. J. Mater. Sci. **41**, 31–52 (2006)
20. G. Burns, F.H. Dacol, Crystalline ferroelectrics with glassy polarization behavior. Phys. Rev. B **28**, 2527–2530 (1983)